Journal Name

COMMUNICATION

Photothermal-triggered release of singlet oxygen from an endoperoxide-containing polymeric carrier for killing cancer cells

Received 00th January 20xx,
Accepted 00th January 20xx

DOI: 10.1039/x0xx00000x

www.rsc.org/

Wen Lv,[a] Huiting Xia,[a] Kenneth Yin Zhang,[a] Zejing Chen,[a] Shujuan Liu,[a] Wei Huang,*[ab] and Qiang Zhao*[a]

A polymeric carrier containing naphthalene and iridium(III) complex was developed to deliver extracellular singlet oxygen ($^1O_2$) into cancer cells to induce the oxidative damage without intracellular O_2 consumption. The release of $^1O_2$ was triggered by the photothermal effect of Au nanorods upon irradiation at 808 nm, realizing a controllable therapy combining both oxidative and photothermal damage.

Singlet oxygen ($^1O_2$), which is one of the reactive oxygen species (ROS), exhibits high cytotoxicity to living cells, and is one of the most important oxidants during cancer treatment.[1] However, the highly reactive $^1O_2$ could not exist in aqueous solution stably (~3.5 μs in H_2O),[2] making the delivery of $^1O_2$ difficult. Photo-induced *in situ* generation of $^1O_2$ through energy transfer from the excited photosensitizers to ground-state oxygen molecules facilitates the enrichment of $^1O_2$ to kill cancer cells, which has been referred to as photodynamic therapy (PDT).[1a-1c]

PDT exerts the therapeutic action in sites where the photosensitizers are photo-excited with specific wavelengths, realizing the light-activated, non-invasive and tumor-specific therapy. These advantages of PDT have attracted significant attentions in biomedical area and promoted the investigations of various photosensitizers for cancer therapy. However, the therapeutic effect of PDT is often restricted by the following aspects: 1) Many of the photosensitizers require ultraviolet-visible (UV-Vis) light excitation, which limits the tissue penetration depth of PDT, and 2) generation of $^1O_2$ requires sufficient supply of O_2, but the solid tumors are hypoxic in nature. To address these challenges, deep PDT techniques have been developed to increase the tissue penetration depth by using favorable excitation sources, including near infrared (NIR) light,[3] X-ray radiation,[4] self-luminescence[5] and ultrasound,[6] to replace the UV-Vis excitation. To improve therapeutic performance under hypoxia, photosensitizers that are capable of enriching intracellular O_2[7,8] or generating ROS in the absence of O_2[9] have been developed. Additionally, we have recently reported a mitochondria-targeted phosphorescent photosensitizer which induced a relatively high intramitochondrial oxygen concentration under hypoxic conditions, thus resulting in an improved PDT effects for hypoxic tumor cells.[10]

Polycyclic aromatic hydrocarbons (such as naphthalene and anthracene) are able to reversibly trap and to thermally release $^1O_2$,[11] which provides new insights into design strategies for delivering $^1O_2$ for the treatment of hypoxic tumor cells.[12] Herein, we synthesized a novel water-soluble polymeric carrier (P1), which could deliver $^1O_2$ effectively (Scheme 1a). The polymer was composed of four components, including a phosphorescent iridium(III) complex, 1,4-dimethyl-naphthalene (DMN), hydrophilic polyethylene glycol (PEG), and a reserved modifiable disulfide group. The iridium(III) complex was served as the phosphorescent indicator to monitor the uptake of polymer and a photosensitizer to generate $^1O_2$. Such cyclometalated complexes, including carboplatin, iridium(III) complex and rhodium(III) complex, would also exhibit chemotherapeutic effect on cancer cells after appropriate modification.[13] The generated $^1O_2$ was trapped by DMN to form endoperoxide (EPO). The release of $^1O_2$ can be triggered by increasing temperature. Compared to 9.10-diphenyl-anthracene, which is another widely-used $^1O_2$ acceptor, DMN allowed easy control of the thermolysis temperature via structural modification at the C2-position of the naphthalene rings, leading to the higher $^1O_2$ generation efficiency.[14] The disulfide group in polymer allowed further functionality for specific purposes. As the iridium(III) complex and DMN were combined in the same polymer chain, the formation of the endoperoxide analogue was quite efficient, affording the $^1O_2$ loaded polymer (P1-SO). To trigger efficient thermolysis in

[a] Key Laboratory for Organic Electronics and Information Displays and Institute of Advanced Materials (IAM)
Nanjing University of Posts and Telecommunications (NUPT)
Nanjing 210023, P. R. China
E-mail: iamqzhao@njupt.edu.cn; wei-huang@njtech.edu.cn
[b] Shaanxi Institute of Flexible Electronics (SIFE)
Northwestern Polytechnical University (NPU)
Xi'an 710072, P. R. China

† Electronic Supplementary Information (ESI) available: [details of any supplementary information available should be included here]. See DOI: 10.1039/x0xx00000x

Please do not adjust margins

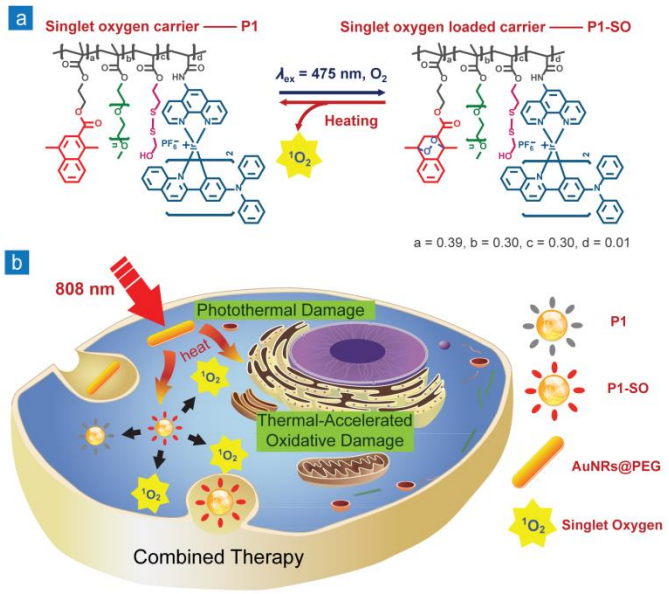

Scheme 1 (a) Mechanism of the reversibly trap and release of $^1O_2$ by the polymeric $^1O_2$ carrier. (b) Illustration of therapy combining both thermal-accelerated oxidative damage and photothermal damage

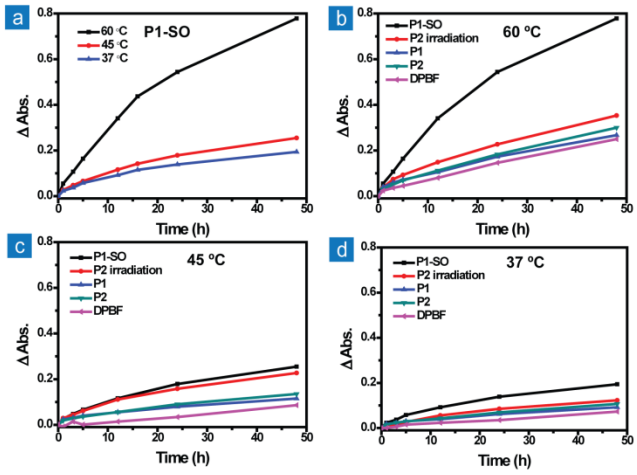

Fig. 1 Δ_{Abs} of DPBF under different conditions in DMSO. The solution of (a) P1-SO (50 μg/mL), photoirradiated P2 (50 μg/mL, λ_{ex} = 475 nm, 55 mW/cm^2, 4 h), P1 (50 μg/mL) and P2 (50 μg/mL) were separately mixed with DPBF (5 ×10^{-5} M). The mixture solution was then heated at (b) 60 °C, (c) 45 °C and (d) 37 °C in dark. The absorption spectra were recorded after different period of heating. The measurements and data collection were conducted at 25 °C.

cancer cells, the cells were coincubated with P1-SO and PEG modified gold nanorods (AuNRs@PEG). Upon NIR irradiation at 808 nm, the photothermal effect of the nanorods not only kills the cells thermally,[15] but also accelerates the release of cytotoxic $^1O_2$ from P1-SO, realizing a photothermal-triggered therapy which combines both oxidative damage and photothermal damage to cancer cells (Scheme 1b).

The $^1O_2$ carrier P1 containing DMN pendants and its DMN-free counterpart P2 were synthesized via radical polymerization (Scheme S1 and S2). Both polymers have been characterized by nuclear magnetic resonance hydrogen (^{1}H NMR) spectra, gel permeation chromatography (GPC), UV-Vis absorption spectra, and emission spectra (Fig. S1-S4). The contents of the iridium(III) complex and DMN in P1 were calculated to be 2.05 w% and 10.12 w%, respectively, through UV-Vis absorption and ^{1}H NMR data. AuNRs@PEG was synthesized through a modified process according to the reported methods.[15]

The capture of $^1O_2$ by DMN can be visualized through the absorption decrease, owing to the formation of EPO (Fig. S5).[14b] Irradiation of P1 in oxygen-saturated DMSO at 475 nm (55 mW/cm^2) at room temperature for 4 h generated P1-SO where DMN was converted into EPO. The $^1O_2$ releasing of P1-SO was investigated under dark conditions at three temperatures, 37 ℃, 45 ℃, and 60 ℃ using 1,3-diphenylisobenzofuran (DPBF) as an indicator, which exhibited a decreasing in absorbance at 417 nm (Δ_{Abs}) in the presence of $^1O_2$. As shown in Fig. 1a, a higher temperature could favor faster and more efficient $^1O_2$ release (Fig. 1). In contrast, the Δ_{Abs} values become much smaller when the endoperoxide-free P1 was used instead of P1-SO (Fig. 1b-1d). Additionally, when DMN-free P2 was used, negligible generation of $^1O_2$ was observed even P2 was preirradiated at 475 nm for 4 h (Fig. 1b-1d). The above results demonstrated that the photoexcitation of P1 could effectively produce P1-SO, which released the cytotoxic $^1O_2$ through thermolysis process, indicating its excellent ability to trap and release $^1O_2$.

Human body develops an elaborated antioxidant defense system to maintain the balance of oxidative stress to protect the cells from disruption by excess ROS.[16] Therefore, sufficient ROS released in a short time, which could break the balance of oxidative stress, will be more effective to induce cell death. In this work, the AuNRs@PEG was used as the photothermal source to facilitate the thermolysis of P1-SO in cancer cells. According to the TEM images, the AuNRs@PEG possessed a uniform structure of rods, which were approximately 55 nm in length and 12 nm in width (Fig. 2a and Fig. S6). The zeta potentials and hydrodynamic sizes of AuNRs and AuNRs@PEG were measured (Table S1). As the unmodified AuNRs were stabilized by the positive surfactant cetyltrimethyl ammonium bromide (CTAB), a positive zeta potential (20.83 ± 2.05 mV) was obtained. The average hydrodynamic size of AuNRs was measured to be 41.1 ± 0.4 nm. After PEG coating, AuNRs@PEG showed the negative zeta potential (-13.30 ± 0.86 mV) and improved average hydrodynamic size (56.9 ± 2.8 nm), demonstrating the successfully coating of PEG on the surface. The UV-vis absorption spectra of AuNRs and AuNRs@PEG exhibited strong absorption peaks in NIR region at around 825 nm (Fig. S7). The peak showed a slight red-shift by approximately 8 nm after PEG coating. To evaluate the photothermal performance of the AuNRs@PEG in aqueous solution, the temperature increase was recorded under continuously exposure to 808 nm laser (0.88 W/cm^2) at both 25 °C and 37 °C. As shown in Fig. 2b and Fig. S8, the temperature of the solutions increased by at least 24 °C upon irradiation for about 15 min, while the temperature increase of the blank solvent was much less, demonstrating the good photothermal effect of AuNRs@PEG.

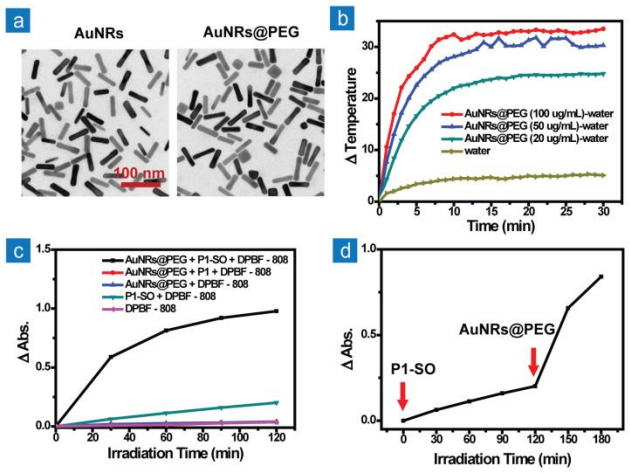

Fig. 2 (a) TEM images of AuNRs and AuNRs@PEG. (b) Temperature increase of the aqueous solution of AuNRs@PEG with different concentrations (100 μg/mL, 50 μg/mL and 20 μg/mL) under 808 nm laser irradiation (0.88 W/cm^2) for 30 min. (c) Δ_{Abs} of the DMSO solution, which mixed AuNRs@PEG (100 μg/mL), P1-SO (200 μg/mL) or P1 (200 μg/mL) with DPBF (5 ×10^{-5} M), under 808 nm light exposure (0.88 W/cm^2) in 2 hours. (d) Δ_{Abs} of the mixture of P1-SO (200 μg/mL) and DPBF (5 ×10^{-5} M) in DMSO under 808 nm light exposure (0.88 W/cm^2) in 2 h. After that, AuNRs@PEG (100 μg/mL) was added and the Δ_{Abs} was continuously recorded under 808 nm light irradiation (0.88 W/cm^2) for the following 1 h. The measurements and data collection were conducted at 25 °C.

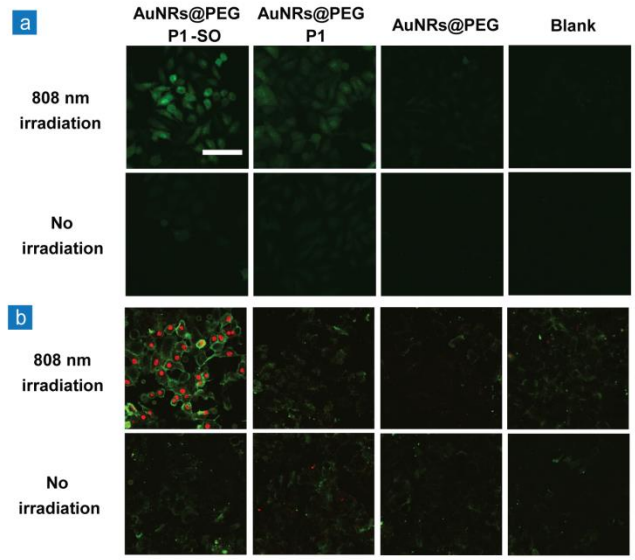

Fig. 3 Confocal microscopy images of HeLa cells treated with (a) DCFH-DA and (b) Annexin V-FITC and PI under different conditions. The cells were incubated with AuNRs@PEG (20 μg/mL) for 24 h and successively incubated with P1-SO (50 μg/mL) or P1 (50 μg/mL) for 6 h at 37 °C. Then the cells were treated with (a) DCFH-DA (10 μM) for 30 min at 37 °C or (b) treated with annexin V-FITC (5 μL) and PI (10 μL) at room temperature for 10 min in dark. Afterwards, the cells were irradiated with 808 nm NIR light (0.88 W/cm^2) for 20 min. The luminescence of DCF was viewed 20 min later in green channel (λ_{ex} = 488 nm, λ_{em} = 500-540 nm). The luminescence of FITC and PI was viewed 7 h later in green channel (λ_{ex} = 488 nm, λ_{em} = 500-560 nm) and red channel (λ_{ex} = 488 nm, λ_{em} = 600-680 nm), respectively. All the images share the same scale bar of 100 μm. Images were taken at 25 °C.

To investigate the release of $^1O_2$ from P1-SO under the photothermal stimulation of AuNRs@PEG, the mixture of P1-SO and AuNRs@PEG was exposed to 808 nm laser irradiation (0.88 W/cm^2) using DPBF as a $^1O_2$ indicator. As shown in Fig. 2c, the mixture displayed an obvious and rapid increase of Δ_{Abs} when prolonged the laser irradiation time, suggestive of an efficient release of $^1O_2$ from P1-SO. In the control experiments, where P1-SO was absent or replaced by P1, Δ_{Abs} of the solution almost remained unchanged. In the absence of AuNRs@PEG, the solution of P1-SO induced a slight increase in Δ_{Abs} (Fig. 2c,d), owing to the slow thermolysis of P1-SO at room temperature. The release rate of $^1O_2$ increased to about 9 times after photothermal triggering, indicating that AuNRs@PEG could effectively facilitate the release of $^1O_2$ from P1-SO under NIR light excitation.

The cytotoxicity of the polymers and AuNRs@PEG toward HeLa cells was measured through the methyl-thiazolyl-tetrazolium (MTT) assay. The viability of the cells incubated with P1 or P1-SO in dark for 24 h remained higher than 92% when the dose concentration was less than 100 μg/mL (Fig. S9a). The AuNRs@PEG treated cells also showed the cell viability higher than 83% at the concentration lower than 20 μg/mL (Fig. S9b), indicating the good biocompatibility of the polymers and AuNRs@PEG. In order to determine the optimum incubation time of the polymer, the time dependent imaging of cells treated with P1 was performed in 24 h (Fig. S10). The intracellular luminescence intensity increased as prolonging the incubation time and remained almost unchanged after 7.5 h, indicating that little amount of polymer would be uptaken by HeLa cells 7.5 h later.

To evaluate the ability of P1-SO and AuNRs@PEG to generate ROS in living cells, 2',7'-dichlorofluorescein diacetate (DCFH-DA) was used as an indicator for intracellular ROS. The non-fluorescent DCFH-DA could be enzymatically hydrolyzed to DCFH by intracellular esterases and further oxidized to green fluorescent DCF by ROS.[17] According to confocal microscopy imaging (Fig. 3a), the HeLa cells coincubated with AuNRs@PEG and P1-SO and then irradiated with 808 nm laser exhibited bright green luminescence of DCF, indicating the generation of intracellular ROS. When removing NIR excitation or AuNRs@PEG treatment, the cells displayed negligible green fluorescence at a physiological temperature of 37 °C (Fig. 3a and S11), owing to the lack of thermal source to facilitate the thermalysis of P1-SO, demonstrating the slowly released $^1O_2$ could hardly induce the generation of intracellular ROS. When removing P1-SO or replacing P1-SO with P1, a weaker fluorescence of DCF could be observed after the NIR laser irradiation, indicating the photothermal damage of Au nanorods could lead to a relatively slow increase of intracellular ROS. Blank cells loaded with DCFH-DA exhibited negligible green fluorescence of DCF no matter whether the cells were irradiated by 808 nm NIR light or not. The above results demonstrated that the photothermal AuNRs@PEG could effectively accelerate the release of $^1O_2$ from P1-SO, leading to both photothermal damage and oxidative damage to cancer cells to facilitate the generation of intracellular ROS.

The therapy performance was further studied through a cell apoptosis assay by using Annexin V-FITC and PI as indicators. Annexin V-FITC and PI could label the apoptotic and dead cells by staining the cell membrane with green fluorescent FITC and nucleus with red fluorescent PI, respectively. The results

showed that cells treated with AuNRs@PEG, P1-SO and irradiated at 808 nm exhibited efficient FITC and PI staining (Fig. 3b). About 25.9% of cells, which was yielded by statistics of more than 700 cells, were killed in 7 hours under the culture condition, indicating the excellent performance of the therapy. The therapy was triggered by the photothermal effect, which will be very practical in the controllable treatment of tumor cells. In the control experiments under the same conditions described in the ROS imaging, the Annexin V staining was less efficient and negligible PI staining was observed (Fig. 3b and S12), which was consistent with the trend of the ROS detection results.

Conclusions

In conclusion, this work aims to overcome the restriction of insufficient oxygen supply and limited penetration depth during the PDT process. Therefore, we developed a novel polymeric $^1O_2$ carrier to deliver the extracellular cytotoxic $^1O_2$ into cancer cells and avoid the intracellular O_2 consumption. The release of $^1O_2$ was trigged by photothermal effect of AuNRs@PEG under NIR light irradiation, realizing the photothermal-controlled oxidative damage and photothermal damage to cancer cells. This strategy effectively accelerated the generation of intracellular ROS and further facilitated the cell death, which exhibited excellent therapeutic effect on cancer cells and would be very promising for tumor therapy. To the best of our knowledge, this work is the first example to develop the multifunctional polymeric carrier for photothermal-triggered release of $^1O_2$ for the treatment of cancer cells. The current limitation of this work is that the polymeric $^1O_2$ carrier P1 and photothermal Au nanorods are two separated agents, because it is difficult to attach enough amount of P1 to the surface of AuNRs. In our next work, we will focus on the integration of two agents into one system by optimizing the amount of polymers attached to AuNRs or designing the polymerizable organic photothermal agents to be incorporated into polymer. In addition, the iridium(III) complex linked to the polymer also exhibits intrinsic cytotoxicity, which is highly related to the dye uptake and distribution,[18] and should be taken into consideration in the future research. These works are undergoing in our laboratory. We believe that the strategy of photothermal-triggered release of $^1O_2$ or other ROS will be an important and urgent research topic in cancer medicine and we hope this work could provide new insights for developing medical materials for tumor therapy.

Acknowledgements

This work was supported by the National Natural Science Foundation of China (51473078, 21501098, and 21671108), National Program for Support of Top-Notch Young Professionals, Scientific and Technological Innovation Teams of Colleges and Universities in Jiangsu Province (TJ215006), Natural Science Foundation of Jiangsu Province of China (BK20150833), Priority Academic Program Development of Jiangsu Higher Education Institutions (YX03001), and the Open Research Fund of State Key Laboratory of Bioelectronics, Southeast University.

Notes and references

1 (a) W. Fan, P. Huang, X. Chen, *Chem. Soc. Rev.*, 2016, **45**, 6488; (b) S. S. Lucky, K. C. Soo, Y. Zhang, *Chem. Rev.*, 2015, **115**, 1990; (c) Z. Zhou, J. Song, L. Nie, X. Chen, *Chem. Soc. Rev.*, 2016, **45**, 6597; (d) J. Liu, W. Bu, J. Shi, *Chem. Rev.*, 2017, **117**, 6160.

2 (a) J. Moan, K. Berg, *Photochem. Photobiol.*, 1991, **53**, 549; (b) S. Hatz, J. D. C. Lambert, P. R. Ogilby, *Photochem. Photobiol. Sci.*, 2007, **6**, 1106; (c) E. Skovsen, J. W. Snyder, J. D. C. Lambert, P. R. Ogilby, *J. Phys. Chem. B*, 2005, **109**, 8570; (d) J. R. Hurst, J. D. McDonald, G. B. Schuster, *J. Am. Chem. Soc.*, 1982, **104**, 2065.

3 (a) C. Wang, H. Tao, L. Cheng, Z. Liu, *Biomaterials*, 2011, **32**, 6145; (b) S. Cui, D. Yin, Y. Chen, Y. Di, H. Chen, Y. Ma, S. Achilefu, Y. Gu, *ACS Nano*, 2013, **7**, 676.

4 H. Chen, G. D. Wang, Y. J. Chuang, Z. Zhen, X. Chen, P. Biddinger, Z. Hao, F. Liu, B. Shen, Z. Pan, J. Xie, *Nano Lett.*, 2015, **15**, 2249.

5 C. Y. Hsu, C. W. Chen, H. P. Yu, Y. F. Lin, P. S. Lai, *Biomaterials*, 2013, **34**, 1204.

6 P. Huang, X. Qian, Y. Chen, L. Yu, H. Lin, L. Wang, Y. Zhu, J. Shi, *J. Am. Chem. Soc.*, 2017, **139**, 1275.

7 Z. Ma, X. Jia, J. Bai, Y. Ruan, C. Wang, J. Li, M. Zhang, X. Jiang, *Adv. Funct. Mater.*, 2017, **27**, 1604258.

8 Y. Cheng, H. Cheng, C. Jiang, X. Qiu, K. Wang, W. Huan, A. Yuan, J. Wu, Y. Hu, *Nat. Commun.*, 2015, **6**, 8785.

9 M. E. Alberto, J. Pirillo, N. Russo, C. Adamo, *Inorg. Chem.*, 2016, **55**, 11185.

10 W. Lv, Z. Zhang, K. Y. Zhang, H. Yang, S. Liu, A. Xu, S. Guo, Q. Zhao, W. Huang, *Angew. Chem. Int. Ed.*, 2016, **55**, 9947.

11 J. M. Aubry, C. Pierlot, J. Rigaudy, R. Schmidt, *Acc. Chem. Res.*, 2003, **36**, 668.

12 S. Kolemen, T. Ozdemir, D. Lee, G. M. Kim, T. Karatas, J. Yoon, E. U. Akkaya, *Angew. Chem. Int. Ed.*, 2016, **55**, 3606.

13 (a) D. Holmes, *Nature*, 2015, **527**, S218; (b) D. L. Ma, L. J. Liu, K. H. Leung, Y. T. Chen, H. J. Zhong, D. S. H. Chan, H. M. D. Wang, C. H. Leung, *Angew. Chem. Int. Ed.*, 2014, **53**, 9178; (c) X. Ma, J. Jia, R. Cao, X. Wang, H. Fei, *J. Am. Chem. Soc.*, 2014, **136**, 17734.

14 (a) M. Klaper, T. Linker, *J. Am. Chem. Soc.*, 2015, **137**, 13744; (b) M. Klaper, T. Linker, *Chem. Eur. J.*, 2015, **21**, 8569.

15 (a) Z. Zhang, L. Wang, J. Wang, X. Jiang, X. Li, Z. Hu, Y. Ji, X. Wu, C. Chen, *Adv. Mater.*, 2012, **24**, 1418; (b) X. Liu, N. Huang, H. Li, H. Wang, Q. Jin, J. Ji, *ACS Appl. Mater. Interfaces*, 2014, **6**, 5657.

16 T. Debevec, G. P. Millet, V. Pialoux, *Front. Physiol.*, 2017, **8**, 84.

17 (a) N. A. Daghastanli, R. Itri, M. S. Baptista, *Photochem. Photobiol.*, 2008, **84**, 1238; (b) P. Bilski, A. G. Belanger, C. F. Chignell, *Free Radical Bio. Med.*, 2002, **33**, 938; (c) P. Wardman, *Free Radical Bio. Med.*, 2007, **43**, 995.

18 (a) C. Caporale, C. A. Bader, A. Sorvina, K. D. M. MaGee, B. W. Skelton, T. A. Gillam, P. J. Wright, P. Raiteri, S. Stagni, J. L. Morrison, S. E. Plush, D. A. Brooks, M. Massi, *Chem. Eur. J.*, 2017, DOI: 10.1002/chem.201701352; (b) C. Dolan, R. D. Moriarty, E. Lestini, M. Devocelle, R. J. Forster, T. E. Keyes, *J. Inorg. Biochem.*, 2013, **119**, 65.

